ACS SyntheticBiology

pubs.acs.org/synthbio Letter

Hyperstable *De Novo* Protein with a Dimeric Bisecting Topology

Naoya Kimura, Kenji Mochizuki, Koji Umezawa, Michael H. Hecht, and Ryoichi Arai*

Cite This: *ACS Synth. Biol.* 2020, 9, 254–259 Read Online

ACCESS | Metrics & More | Article Recommendations | Supporting Information

ABSTRACT: Recently, we designed and assembled protein nanobuilding blocks (PN-Blocks) from an intermolecularly folded dimeric *de novo* protein called WA20. Using this dimeric 4-helix bundle, we constructed a series of self-assembling supramolecular nanostructures including polyhedra and chain-type complexes. Here we describe the stabilization of WA20 by designing mutations that stabilize the helices and hydrophobic core. The redesigned proteins denature with substantially higher midpoints, with the most stable variant, called Super WA20 (SUWA), displaying an extremely high midpoint (T_m = 122 °C), much higher than the T_m of WA20 (75 °C). The crystal structure of SUWA reveals an intermolecularly folded dimer with bisecting U topology, similar to the parental WA20 structure, with two long α-helices of a protomer intertwined with the helices of another protomer. Molecular dynamics simulations demonstrate that the redesigned hydrophobic core in the center of SUWA significantly suppresses the deformation of helices observed in the same region of WA20, suggesting this is a critical factor stabilizing the SUWA structure. This hyperstable *de novo* protein is expected to be useful as nanoscale pillars of PN-Block components in new types of self-assembling nanoarchitectures.

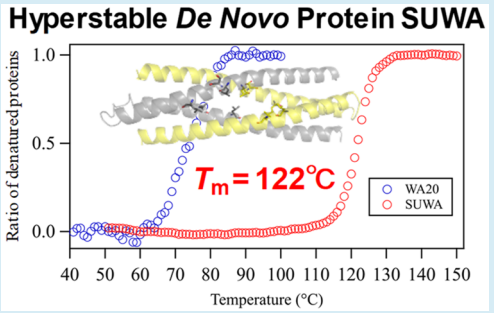

KEYWORDS: *protein stabilization, de novo protein, binary pattern, 4-helix bundle, bisecting U topology, protein nanobuilding block*

The chemical reconstitution of living matter is one of the ultimate goals of chemistry and synthetic biology. Toward achieving this goal, the design of artificial proteins—and the programmed self-assembly of such proteins into complex and nanostructures—are important steps in the emerging field of "synthetic structural biology".[1,2]

As a semirational approach toward protein design, the binary code strategy was developed to construct libraries of novel polypeptides that would fold into predetermined structures. Using secondary structure motifs with binary patterns of polar and nonpolar residues, *de novo* proteins with α-helixes or β-sheets have been successfully created without reference to natural protein sequences.[3] From a third-generation library of binary patterned 4-helix bundles, several *de novo* proteins with functions *in vitro*[4,5] and *in vivo*[6−9] have been produced.

We reported the crystal structure of WA20, a protein from the third-generation library of binary patterned 4-helix bundles,[4,10] which forms an intermolecularly folded dimeric helical bundle (so-called dimeric "nunchaku"-like structure).[11] To harness the unusual intertwined structure of WA20 for the self-assembly of supramolecular nanostructures, we designed and constructed a polyhedral protein nanobuilding block (PN-Block), called "WA20-foldon" by fusing the dimeric *de novo* protein WA20 to a trimeric foldon domain of T4 phage fibritin.[12] The WA20-foldon formed several distinctive types of self-assembled nanoarchitectures including combinations of dimers and trimers in multiples of 6-mers, which formed a barrel-like hexamer and a tetrahedrally shaped dodecamer.

The overall objective of the "PN-Block strategy" is to construct a wide range of self-assembling nanostructures from a few types of simple and fundamental PN-Blocks. The intertwined rod-like structure of the *de novo* protein WA20, with its intermolecularly folded dimeric structure, is well suited as a simple and versatile PN-Block for the design and construction of a range of different nanoarchitectures.[12]

Recently, we designed and created a new class of *de novo* nanobuilding blocks, which we called extender protein nanobuilding blocks (ePN-Blocks).[13] These were constructed by joining tandemly two copies of WA20 with various linkers. These linked proteins enabled the construction of a new series of PN-Blocks that self-assembled into cyclized and extended chain-type nanostructures. We successfully reconstructed heteromeric complexes from extender and stopper PN-Blocks, and the complexes further self-assembled into supramolecular nanostructures.[13]

With the long-term goal of producing nanostructures with extremely high stabilities for applications in nanotechnology, we were motivated to stabilize WA20, the central component of these nanostructures. The current study describes the successful stabilization of WA20 by rational design of mutations that stabilize the helices and hydrophobic core.

Received: December 9, 2019
Published: January 17, 2020

https://dx.doi.org/10.1021/acssynbio.9b00501
ACS Synth. Biol. 2020, 9, 254–259

RESULTS AND DISCUSSION

In the WA20 structure (Figure 1), position 28 near the center of the first α-helix is occupied by a glycine residue. Since

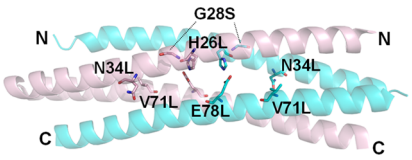

Figure 1. Mutations designed to stabilize the *de novo* protein WA20. Side chains of the original sequence are shown as sticks in the crystal structure of WA20 (PDB: 3VJF).[11] Chains A and B are shown in magenta and cyan, respectively.

glycine has the lowest helix propensity of any amino acid,[14] we replaced this residue. Because residue 28 occurs on the solvent exposed face of the helix, we replaced Gly28 with serine, a polar residue.

Next, we sought to stabilize the buried core of WA20. On the basis of the crystal structure of WA20 (PDB: 3VJF),[11] we focused on His26, Asn34, Val71, and Glu78 (Figure 1 and Figure S1, Supporting Information).

Residues His26 and Glu78 are located in the core near the middle of the α-helices, and pairs of these residues form intrachain hydrogen bonds (or salt bridges) (Figure S1A). These buried polar residues are inconsistent with the binary patterning strategy—which populates the core with hydrophobic residues and places polar residues on the surface—because they were originally designed to form an interhelical loop in a monomeric 4-helix bundle.[4] We mutated both His26 and Glu78 to leucine, which has a high helix propensity[14] and would be expected to promote nonpolar helix−helix interactions, as seen in many structures related to leucine zippers and coiled coils.[15]

Val71 is located at a hydrophobic pocket on the surface of WA20 (Figure S1B). The mutation of Val71 to leucine was designed to fill the pocket.

Finally, Asn34 is located at helix−helix interface (Figure S1C). The mutation of Asn34 to leucine was designed to stabilize the helix−helix interface by incorporating a hydrophobic interaction.

All of the mutant proteins expressed well in *Escherichia coli*, and were purified by immobilized metal ion affinity chromatography. Circular dichroism (CD) spectra at 30 °C showed that all variants formed α-helical structures as well as the parental WA20 protein (Figures 2A and S2). Thermal denaturation revealed that all variants had higher midpoint temperatures (T_m) than WA20 (Table 1 and Figure S3). The single mutations G28S, N34L, and V71L each improved the T_m by 8, 10, and 9 °C, respectively, compared to WA20 (T_m = 75 °C). The double mutant H26L/E78L enhanced thermal stability substantially with ΔT_m = 26 °C. The variant with all five mutations (H26L/G28S/N34L/V71L/E78L) (Figure S4), called Super WA20 (SUWA), achieved a remarkable improvement in stability with T_m = 122 °C, 47 °C higher than the parental protein (Figure 2A and 2B and Table 1). In addition, the thermal denaturation curves of WA20 and SUWA showed a two-state unfolding transition (Figure 2B), but the other WA20 variants (H26L/E78L, G28S, N34L, and V71L) seemed to show a three-state unfolding transition (Figure S3A), suggesting that there are some intermediate states in unfolding processes of these WA20 variants. The observed T_m values may

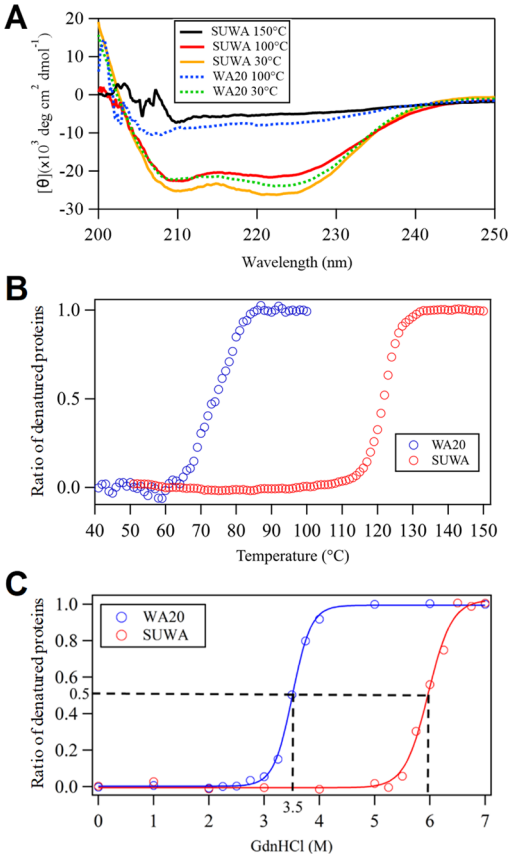

Figure 2. Secondary structure and stability of the *de novo* protein WA20 and SUWA (Super WA20). (A) Circular dichroism (CD) spectra of WA20 and SUWA. (B) Thermal denaturation curves of WA20 and SUWA. $[\theta]_{222\ nm}$ measured by CD is normalized and plotted as a function of temperature. (C) Chemical denaturation of WA20 and SUWA as a function of guanidine hydrochloride (GdnHCl).

Table 1. Denaturation Midpoint Temperature (T_m) of WA20 and Its Variants

WA20	G28S	N34L	V71L	H26L/E78L	SUWA
75 °C	83 °C	85 °C	84 °C	101 °C	122 °C

depend on protein concentration because the stability of a dimeric protein depends on protein concentration when the dimer unfolds into two monomers.

Furthermore, SUWA was stabilized substantially against chemical denaturation by guanidine hydrochloride (GdnHCl). The denaturation midpoint concentration (C_m) of SUWA was increased to 6 M GdnHCl, compared to WA20 (C_m = 3.5 M GdnHCl) (Figure 2C). Assuming that the chemical denaturation was a two-state transition between folded and unfolded states, the folding free energy (ΔG_F) of SUWA and WA20 were estimated to be −29.6 kcal/mol and −22.8 kcal/mol, respectively (Figure S5).[16]

Size exclusion chromatography−multiangle light scattering (SEC−MALS) analysis showed that SUWA formed a dimer (M_w = 24.8 kDa) as well as WA20 (Table S1 and Figure S6). Small-angle X-ray scattering (SAXS) also indicated that SUWA formed a dimer (M_w = 23.8 kDa) and an elongated structure (the maximum diameter, D_{max} = 10 nm) as was the case with WA20 (Table S2 and Figure S7).

https://dx.doi.org/10.1021/acssynbio.9b00501
ACS Synth. Biol. 2020, 9, 254−259

We solved the crystal structure of SUWA (Figure 3 and Table S3) at 2.0 Å resolution, revealing an intermolecularly

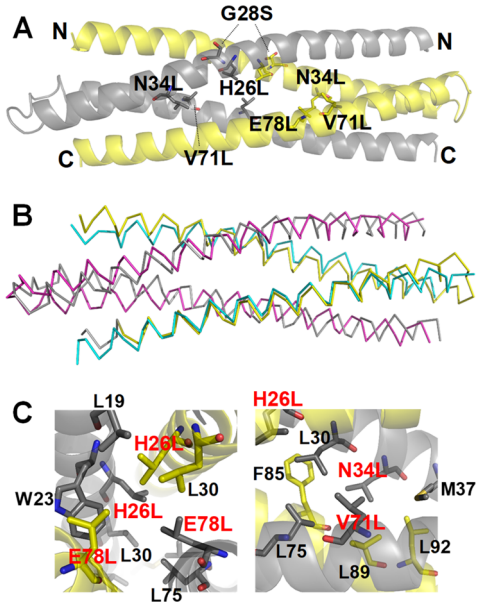

Figure 3. Crystal structure of SUWA. (A) Ribbon representation of the overall structure of SUWA. Mutated residues are shown as stick models. Chains A and B are shown in gray and yellow, respectively. (B) Superimposition of the main-chain structures (C_α) of SUWA and WA20 (RMSD: 2.3 Å). Chains A and B of SUWA are shown in gray and yellow, respectively. Chains A and B of WA20 are shown in magenta and cyan, respectively. (C) Closeup views of the mutation sites of SUWA at the enhanced hydrophobic core.

folded dimer with a bisecting U topology.[17,18] As was the case for the original WA20 structure, SUWA contains two long α-helices of one protomer intertwined with the helices of the other protomer (Figure 3A). There are two dimers of SUWA per asymmetric unit, and the main-chain structures of the α-helices superimpose well (Figure S8A) but not completely (root-mean-square deviation (RMSD) of C_α atoms in α-helices: 1.2 Å for the two dimers of SUWA in an asymmetric unit), suggesting that the structure may be slightly dynamic in solution. The SUWA structure resembles the topology and overall structure of WA20 (Figures 3B and S8B) (RMSD of C_α atoms in α-helices: 2.3 Å for WA20 and SUWA (chains A and B) and 1.7 Å for WA20 and SUWA (chains C and D)). The hydrophobic cores of SUWA were enhanced by the mutations (Figures 3C and S8C).

To further probe how the designed mutations stabilize SUWA relative to WA20, we performed molecular dynamics (MD) simulations for the dimer dissolved in water. We evaluated the probability of forming α-helical structure for each residue of WA20 and SUWA at 310 and 400 K (Figures 4A and S9). In the case of WA20, the α-helical structure at Glu78 and its neighbors were less stable than the other helical regions. The time-dependent trajectories demonstrated that the side chain of Glu78 dynamically flipped to become exposed to solvent (Figure 4B and Movies S1 and S2), which was not found in the static structure of WA20 in the crystal. In response to this side chain movement, several water molecules invaded the central core to fill the vacancy (see meshed region in Figure 4B). The α-helical structures around Glu78 was further destroyed with increasing temperature to 400 K

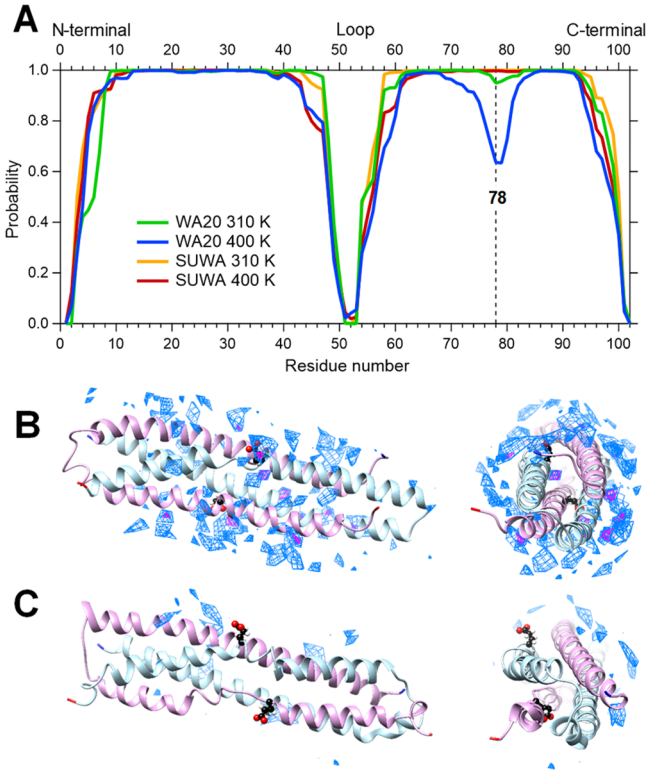

Figure 4. Computational evaluation of the structural stabilities of WA20 and SUWA by MD simulation. (A) Probability of forming α-helical structure for each residue in the dimerized WA20 and SUWA proteins in aqueous solution at 310 and 400 K. A probability of 1.0 indicates that the α-helical structure is preserved over the simulation. The graphs including error bars are shown in Figure S9. (B) A typical snapshot of the partially unfolded WA20 dimer observed at 310 K. The atoms in Glu78 are represented by sticks and balls. The meshes indicate the local regions where the density of water molecules is 4 times higher (purple mesh) and 3 times higher (light blue mesh) than bulk. The right image corresponds to the axial view of the left one. (C) A typical snapshot of the partially unfolded the WA20 dimer observed at 400 K. The light blue meshes indicate the local regions where the density of water molecules is 3 times higher than bulk. The right image corresponds to the axial view of the left one.

(Figure 4C and Movie S3), suggesting that the unstable conformations around Glu78 are related to the thermal unfolding of WA20.

In contrast to these dynamic features in WA20, MD simulations of SUWA revealed that the α-helix around Leu78 was stabilized significantly—even at the higher temperature of 400 K (Figure 4A and Movie S4). Moreover, the Leu78 side chain stayed buried inside SUWA dimer and no interstitial water molecules were observed in contrast to WA20. These MD simulations indicate that the stabilized α-helical structure with the enhanced hydrophobic core at the center of SUWA eliminates one of the triggers for unfolding, thereby making SUWA significantly more stable than WA20.

For many years, the stabilization of various proteins has been studied in the fields of protein engineering and design.[19−27] Recent years have seen the design of several hyperstable *de novo* proteins. For example, Huang *et al.* described parametrically designed helical bundles with high thermodynamic stability[28] and Hsia *et al.* reported a hyperstable 60-subunit icosahedron complex.[29] With increasing understanding of the factors underpinning protein design and stability,[30] it is now

https://dx.doi.org/10.1021/acssynbio.9b00501
ACS Synth. Biol. 2020, 9, 254−259

possible to consider applications of *de novo* designed hyperstable proteins. These considerations motivated the current effort to enhance the stability of WA20, the central component of our PN-Blocks.[12,13] The newly designed variant, SUWA, has several key advantages for applications in various fields such as synthetic biology and nanotechnology: It is small and simple; it expresses well in *E. coli*; its intertwined rod-like dimeric structure can nucleate a range of topologies that are not accessible to monomeric 4-helix bundles; and as a result of the current work, it is extremely stable, maintaining its folded structure well at temperatures above the boiling point of water or at 5 M GdnHCl. Moreover, a series of the *de novo* proteins with a variety of stability are also potentially useful for the programmable design and assembly of nanoarchitecture frameworks as nanoscale pillars of PN-Blocks contributing to synthetic biology. Because SUWA was derived from a sequence (WA20) taken from a vast library of binary patterned helical bundles,[4] this protein is merely the first of many PN-Block components that could eventually be used in the design of self-assembling protein nanoarchitectures. Additionally, our previous demonstration that binary patterned proteins possess a range of binding and catalytic properties (*in vitro*[4,5] and *in vivo*[6−9]) suggests that this system may ultimately provide PN-Blocks for the design of functional nanomaterials.

METHODS

Construction of Protein Expression Plasmids. Protein expression plasmids of the WA20 variants were prepared by targeted site-directed mutagenesis of the plasmid pET3a-WA20[11] using the Transfer-PCR method[31] with the oligo-DNA primers (Table S4) and KOD-Plus-Neo DNA polymerase (Toyobo, Osaka, Japan). The amino acid sequences of the WA20 and SUWA proteins are shown in Figure S4.

Protein Expression and Purification. The WA20 and its variant proteins were expressed in *E. coli* BL21 Star (DE3) (Invitrogen, Carlsbad, CA) harboring the expression plasmid in 2 L of LB broth, Lennox (Nacalai Tesque, Kyoto, Japan) containing 50 μg/mL ampicillin sodium salt at 30 °C for 16 h. All proteins were well expressed in *E. coli* without IPTG induction. Proteins were extracted from harvested cells by the freeze−thaw method and sonication with VC 505 Ultrasonic Processor (Sonics and Materials, Newtown, CT) in lysis buffer containing 50 mM sodium phosphate buffer (pH 7.0), 300 mM NaCl, and 10% glycerol. Proteins were purified using immobilized metal affinity chromatography (IMAC) with COSMOGEL His-Accept (Nacalai Tesque). The equilibration/wash buffer contained 50 mM sodium phosphate buffer (pH 7.0) and 300 mM NaCl, and the elution buffer contained 50 mM sodium phosphate buffer (pH 7.0), 300 mM NaCl, 10% glycerol, and 250 mM imidazole. Since many histidine residues are exposed on the surface of the WA20 structure,[11] the WA20 and its variant proteins can bind the IMAC column without a His-tag. Protein concentration was determined by absorbance at 280 nm with molar extinction coefficient of 6760.2 M^{-1} cm^{-1} for WA20 and SUWA as calculated according to the amino acid sequences.

Circular Dichroism (CD) Spectroscopy. For thermal denaturation experiments, we used a J-720 spectropolarimeter (JASCO, Hachioji, Tokyo, Japan) specially equipped with a programmable temperature controller and a pressure-proof cell compartment that prevented the aqueous solution from boiling and evaporating at high temperatures. Thermal denaturation was monitored at ellipticity $\theta_{222\ nm}$ of a typical peak for α-helices of proteins using the cell compartment pressured by nitrogen gas (+0.5 MPa). Each protein (~0.25 mg/mL) was dissolved in 20 mM sodium phosphate buffer (pH 7.5) containing 150 mM NaCl and 10% glycerol. A cell with 0.1 cm path length was used. The temperature was increased at a rate of 1.0 °C/min. For chemical denaturation experiments, a J-1500 spectropolarimeter (JASCO) was used. The WA20 and SUWA proteins were dissolved in 20 mM sodium phosphate buffer (pH 7.5) containing 150 mM NaCl, 10% glycerol, and 0−7 M guanidine hydrochloride (GdnHCl).

Structural Analyses. The SUWA protein was further purified by cation exchange chromatography and size exclusion chromatography (SEC) (Figure S10) for crystallization. Rod-like crystals (Figure S11A) were obtained in a drop composed of the protein solution (20 mg/mL) and the reservoir solution (0.1 M HEPES, 25% w/v polyethylene glycol 3,350, pH 7.5) at 20 °C by the sitting drop vapor diffusion method. X-ray diffraction data (Figure S11B) were collected at the Photon Factory BL-5A beamline (KEK, Tsukuba, Japan). The SUWA structure was solved by the molecular replacement method with the WA20 structure (PDB ID: 3VJF)[11] as a search model. More detailed methods for X-ray crystallography, small-angle X-ray scattering (SAXS), and SEC−multiangle light scattering (SEC−MALS) were described in Supporting Information.

Molecular Dynamics (MD) Simulations. The all-atom MD simulations were performed using the GPU accelerated AMBER18.[32] The initial coordinate of the WA20 dimer was referred from its crystal structure (PDB ID: 3VJF), and the missing amino acids in the structure were added by using MODELLER.[33] The initial structure of the SUWA dimer was modeled based on the WA20 structure by MODELLER. The *ff14SB* AMBER force field[34] is used to represent these proteins and TIP3P[35] for water. Each of the WA20 and SUWA dimers was dissolved in an octahedral box comprising of 42580 and 39926 water molecules, respectively. Potassium and chloride ions were added to each box to neutralize the total charge as well as to set the ion density equal to 100 mM. The periodic boundary conditions were applied for all directions. The time step of the simulations was 2 fs. After energy minimization, the solution was monotonically heated up from 0 to 310 K for 1 ns under the constant volume, followed by the constant-volume and constant-temperature (*NVT*) MD simulation at 310 K for 1 ns. To equilibrate the volume, the constant-pressure and constant-temperature (*NPT*) MD simulation was performed at 1 bar and 310 K for 1 ns. The equilibrated configuration was finally obtained after performing a 10 ns *NVT*-MD simulation at 310 K. Then, the five different production *NVT*-MD simulations were performed at 310 K for each 500 ns by giving different momenta to the same equilibrated configuration. The production *NVT*-MD simulations at 400 K were prepared in the same way. The trajectories were recorded every 10 ps for analyses. We identified the formation of α-helices based on backbone amide and carbonyl atom positions.[36] Each protomer in a dimer is essentially identical, so we computed the probability of forming α-helical structure for each residue in the respective protomer and took the average between two protomers.

ASSOCIATED CONTENT

Supporting Information

The Supporting Information is available free of charge at https://pubs.acs.org/doi/10.1021/acssynbio.9b00501.

https://dx.doi.org/10.1021/acssynbio.9b00501
ACS Synth. Biol. 2020, 9, 254−259

Supplementary Methods, Supplementary Tables S1−S3, Supplementary Figures S1−S11 (PDF)
Movies S1−S4 (ZIP)

AUTHOR INFORMATION

Corresponding Author

Ryoichi Arai − *Department of Biomolecular Innovation, Institute for Biomedical Sciences, Interdisciplinary Cluster for Cutting Edge Research, Shinshu University, Matsumoto, Nagano 390-8621, Japan; Department of Supramolecular Complexes, Research Center for Fungal and Microbial Dynamism, Shinshu University, Minamiminowa, Nagano 399-4598, Japan; Department of Applied Biology, Faculty of Textile Science and Technology, Shinshu University, Ueda, Nagano 386-8567, Japan;* orcid.org/0000-0001-5606-8483; Email: rarai@shinshu-u.ac.jp

Authors

Naoya Kimura − *Department of Applied Biology, Faculty of Textile Science and Technology, Shinshu University, Ueda, Nagano 386-8567, Japan*

Kenji Mochizuki − *Department of Chemistry and Materials, Faculty of Textile Science and Technology and Institute for Fiber Engineering, Shinshu University, Ueda, Nagano 386-8567, Japan*

Koji Umezawa − *Department of Biomedical Engineering, Graduate School of Science and Technology, Shinshu University, Minamiminowa, Nagano 399-4598, Japan; Institute for Biomedical Sciences, Interdisciplinary Cluster for Cutting Edge Research, Shinshu University, Matsumoto, Nagano 390-8621, Japan*

Michael H. Hecht − *Department of Chemistry, Princeton University, Princeton, New Jersey 08544, United States*

Complete contact information is available at: https://pubs.acs.org/10.1021/acssynbio.9b00501

Notes

The authors declare no competing financial interest.
Atomic coordinates and structure factors of the SUWA structure are available from the worldwide Protein Data Bank (wwPDB) with the accession code 6KOS. The SAXS data and dummy-atom models of WA20 and SUWA are available from Small Angle Scattering Biological Data Bank (SASBDB) with the accession codes, SASDHW3 for WA20 and SASDHX3 for SUWA.

ACKNOWLEDGMENTS

We sincerely thank Prof. Akihiko Yamagishi, Dr. Sota Yagi, and Mr. Takahiro Sasamoto at Tokyo University of Pharmacy and Life Sciences and Prof. Satoshi Akanuma at Waseda University for help in CD experiments; Dr. Takahiro Kosugi, Dr. Rie Koga, and Dr. Nobuyasu Koga at Institute for Molecular Science (IMS) for assistance in SEC−MALS and CD experiments; Dr. Naoya Kobayashi at IMS, and Prof. Takaaki Sato, Mr. Kouichi Inano, and Dr. Keiichi Yanase at Shinshu University for help in SAXS analysis; Mr. Yusuke Koyanagi at Shinshu University and Dr. Keitaro Yamashita at University of Tokyo for help in installing MR-Rosetta. The synchrotron X-ray experiments were performed at Photon Factory (PF), KEK, under the approval of PF program advisory committee (Proposal No. 2014G111, 2014G673, 2016G153, 2016G606, 2016G617, 2018G634, and 2018G636). We thank the beamline scientists and staff at PF, KEK. This work was supported by JSPS KAKENHI Grant numbers JP16K05841, JP16H00761, JP24780097, JP17KK0104, and JP19H02522. This work was also supported by Joint Research program of IMS and JSPS Invitational Fellowship.

REFERENCES

(1) Arai, R. (2018) Hierarchical design of artificial proteins and complexes toward synthetic structural biology. *Biophys. Rev. 10*, 391−410.
(2) Kobayashi, N., and Arai, R. (2017) Design and construction of self-assembling supramolecular protein complexes using artificial and fusion proteins as nanoscale building blocks. *Curr. Opin. Biotechnol. 46*, 57−65.
(3) Hecht, M. H., Das, A., Go, A., Bradley, L. H., and Wei, Y. (2004) De novo proteins from designed combinatorial libraries. *Protein Sci. 13*, 1711−1723.
(4) Patel, S. C., Bradley, L. H., Jinadasa, S. P., and Hecht, M. H. (2009) Cofactor binding and enzymatic activity in an unevolved superfamily of de novo designed 4-helix bundle proteins. *Protein Sci. 18*, 1388−1400.
(5) Cherny, I., Korolev, M., Koehler, A. N., and Hecht, M. H. (2012) Proteins from an unevolved library of de novo designed sequences bind a range of small molecules. *ACS Synth. Biol. 1*, 130−138.
(6) Fisher, M. A., McKinley, K. L., Bradley, L. H., Viola, S. R., and Hecht, M. H. (2011) De novo designed proteins from a library of artificial sequences function in *Escherichia coli* and enable cell growth. *PLoS One 6*, No. e15364.
(7) Digianantonio, K. M., and Hecht, M. H. (2016) A protein constructed de novo enables cell growth by altering gene regulation. *Proc. Natl. Acad. Sci. U. S. A. 113*, 2400−2405.
(8) Digianantonio, K. M., Korolev, M., and Hecht, M. H. (2017) A non-natural protein rescues cells deleted for a key enzyme in central metabolism. *ACS Synth. Biol. 6*, 694−700.
(9) Donnelly, A. E., Murphy, G. S., Digianantonio, K. M., and Hecht, M. H. (2018) A de novo enzyme catalyzes a life-sustaining reaction in *Escherichia coli*. *Nat. Chem. Biol. 14*, 253.
(10) Bradley, L. H., Kleiner, R. E., Wang, A. F., Hecht, M. H., and Wood, D. W. (2005) An intein-based genetic selection allows the construction of a high-quality library of binary patterned de novo protein sequences. *Protein Eng., Des. Sel. 18*, 201−207.
(11) Arai, R., Kobayashi, N., Kimura, A., Sato, T., Matsuo, K., Wang, A. F., Platt, J. M., Bradley, L. H., and Hecht, M. H. (2012) Domain-swapped dimeric structure of a stable and functional de novo four-helix bundle protein, WA20. *J. Phys. Chem. B 116*, 6789−6797.
(12) Kobayashi, N., Yanase, K., Sato, T., Unzai, S., Hecht, M. H., and Arai, R. (2015) Self-assembling nano-architectures created from a protein nano-building block using an intermolecularly folded dimeric *de novo* protein. *J. Am. Chem. Soc. 137*, 11285−11293.
(13) Kobayashi, N., Inano, K., Sasahara, K., Sato, T., Miyazawa, K., Fukuma, T., Hecht, M. H., Song, C., Murata, K., and Arai, R. (2018) Self-assembling supramolecular nanostructures constructed from *de novo* extender protein nanobuilding blocks. *ACS Synth. Biol. 7*, 1381−1394.
(14) Pace, C. N., and Scholtz, J. M. (1998) A helix propensity scale based on experimental studies of peptides and proteins. *Biophys. J. 75*, 422−427.
(15) Lupas, A. (1996) Coiled coils: new structures and new functions. *Trends Biochem. Sci. 21*, 375−382.
(16) Greenfield, N. J. (2006) Determination of the folding of proteins as a function of denaturants, osmolytes or ligands using circular dichroism. *Nat. Protoc. 1*, 2733−2741.
(17) Hill, R. B., and DeGrado, W. F. (1998) Solution structure of α_2D, a nativelike de novo designed protein. *J. Am. Chem. Soc. 120*, 1138−1145.

(18) Glykos, N. M., Cesareni, G., and Kokkinidis, M. (1999) Protein plasticity to the extreme: changing the topology of a 4-α-helical bundle with a single amino acid substitution. *Structure 7*, 597−603.
(19) Hecht, M. H., Sturtevant, J. M., and Sauer, R. T. (1986) Stabilization of lambda repressor against thermal denaturation by site-directed Gly → Ala changes in alpha-helix 3. *Proteins: Struct., Funct., Genet. 1*, 43−46.
(20) Russell, R. J., and Taylor, G. L. (1995) Engineering thermostability: lessons from thermophilic proteins. *Curr. Opin. Biotechnol. 6*, 370−374.
(21) Hill, R. B., Raleigh, D. P., Lombardi, A., and Degrado, W. F. (2000) De novo design of helical bundles as models for understanding protein folding and function. *Acc. Chem. Res. 33*, 745−754.
(22) Lehmann, M., and Wyss, M. (2001) Engineering proteins for thermostability: the use of sequence alignments versus rational design and directed evolution. *Curr. Opin. Biotechnol. 12*, 371−375.
(23) Wijma, H. J., Floor, R. J., and Janssen, D. B. (2013) Structure- and sequence-analysis inspired engineering of proteins for enhanced thermostability. *Curr. Opin. Struct. Biol. 23*, 588−594.
(24) Yu, H. R., and Huang, H. (2014) Engineering proteins for thermostability through rigidifying flexible sites. *Biotechnol. Adv. 32*, 308−315.
(25) Magliery, T. J. (2015) Protein stability: computation, sequence statistics, and new experimental methods. *Curr. Opin. Struct. Biol. 33*, 161−168.
(26) Goldenzweig, A., Goldsmith, M., Hill, S. E., Gertman, O., Laurino, P., Ashani, Y., Dym, O., Unger, T., Albeck, S., Prilusky, J., Lieberman, R. L., Aharoni, A., Silman, I., Sussman, J. L., Tawfik, D. S., and Fleishman, S. J. (2016) Automated structure- and sequence-based design of proteins for high bacterial expression and stability. *Mol. Cell 63*, 337−346.
(27) Zimmerman, M. I., Hart, K. M., Sibbald, C. A., Frederick, T. E., Jimah, J. R., Knoverek, C. R., Tolia, N. H., and Bowman, G. R. (2017) Prediction of new stabilizing mutations based on mechanistic insights from Markov state models. *ACS Cent. Sci. 3*, 1311−1321.
(28) Huang, P. S., Oberdorfer, G., Xu, C., Pei, X. Y., Nannenga, B. L., Rogers, J. M., DiMaio, F., Gonen, T., Luisi, B., and Baker, D. (2014) High thermodynamic stability of parametrically designed helical bundles. *Science 346*, 481−485.
(29) Hsia, Y., Bale, J. B., Gonen, S., Shi, D., Sheffler, W., Fong, K. K., Nattermann, U., Xu, C., Huang, P. S., Ravichandran, R., Yi, S., Davis, T. N., Gonen, T., King, N. P., and Baker, D. (2016) Design of a hyperstable 60-subunit protein icosahedron. *Nature 535*, 136−139.
(30) Baker, D. (2019) What has de novo protein design taught us about protein folding and biophysics? *Protein Sci. 28*, 678−683.
(31) Erijman, A., Dantes, A., Bernheim, R., Shifman, J. M., and Peleg, Y. (2011) Transfer-PCR (TPCR): a highway for DNA cloning and protein engineering. *J. Struct. Biol. 175*, 171−177.
(32) Case, D. A., Ben-Shalom, I. Y., Brozell, S. R., Cerutti, D. S., Cheatham, I. T. E., Cruzeiro, V. W. D., Darden, T. A., Duke, R. E., Ghoreishi, D., Gilson, M. K., Gohlke, H., Goetz, A. W., Greene, D., Harris, R., Homeyer, N., Izadi, S., Kovalenko, A., Kurtzman, T., Lee, T. S., LeGrand, S., Li, P., Lin, C., Liu, J., Luchko, T., Luo, R., Mermelstein, D. J., Merz, K. M., Miao, Y., Monard, G., Nguyen, C., Nguyen, H., Omelyan, I., Onufriev, A., Pan, F., Qi, R., Roe, D. R., Roitberg, A., Sagui, C., Schott-Verdugo, S., Shen, J., Simmerling, C. L., Smith, J., Salomon-Ferrer, R., Swails, J., Walker, R. C., Wang, J., Wei, H., Wolf, R. M., Wu, X., Xiao, L., York, D. M., and Kollman, P. A. (2018) *AMBER 2018*, University of California, San Francisco.
(33) Webb, B., and Sali, A. (2014) Comparative protein structure modeling using MODELLER. *Curr. Protoc. Bioinformatics 47*, 5−6.
(34) Maier, J. A., Martinez, C., Kasavajhala, K., Wickstrom, L., Hauser, K. E., and Simmerling, C. (2015) ff14SB: Improving the accuracy of protein side chain and backbone parameters from ff99SB. *J. Chem. Theory Comput. 11*, 3696−3713.
(35) Jorgensen, W. L., Chandrasekhar, J., Madura, J. D., Impey, R. W., and Klein, M. L. (1983) Comparison of simple potential functions for simulating liquid water. *J. Chem. Phys. 79*, 926−935.
(36) Kabsch, W., and Sander, C. (1983) Dictionary of protein secondary structure: pattern recognition of hydrogen-bonded and geometrical features. *Biopolymers 22*, 2577−2637.

https://dx.doi.org/10.1021/acssynbio.9b00501
ACS Synth. Biol. 2020, 9, 254−259